Sedimentation of particles in a vigorously convecting fluid

G. Lavorel and M. Le Bars*

Institut de Recherche sur les Phénomènes Hors Équilibre, UMR 6594, CNRS and Aix-Marseille Université, 49 Rue F. Joliot Curie, BP 146, F-13384 Marseille Cedex 13, France

(Received 23 February 2009; revised manuscript received 17 July 2009; published 30 October 2009)

The sedimentation of particles in a vigorously convecting fluid is a process of great interest in various geophysical and industrial settings. Using a classical Rayleigh-Bénard setup with salty water as a working fluid and PMMA particles, we systematically quantify the progressive settling of a large number of heavy particles initially distributed homogeneously through the tank. Our two control parameters are the Rayleigh number Ra characterizing the vigor of convection and the density ratio between the particles and the fluid $\frac{\Delta\rho}{\rho}$. In all our experiments, the time evolution of the solid fraction of suspended particles is correctly described by a diffusion-convection equation, taking into account a constant settling velocity given by the classical Stoke's law with an apparent viscosity due to small-scale turbulent motions, as well as a time-independent diffusive flux of particles from the bottom of the tank. We define scaling laws for this diffusive flux as well as for the equilibrium value of the suspended particles solid fraction as a function of Ra and $\frac{\Delta\rho}{\rho}$, in agreement with the experimental results.

DOI: 10.1103/PhysRevE.80.046324 PACS number(s): 47.55.P−

I. INTRODUCTION

The sedimentation of particles in a convecting fluid is a process of great interest in geophysics. This mechanism takes place, for instance, in the atmosphere, where convective motions are involved in the dispersion of polluting particles. A systematic study of this problem is also fundamental to understand the crystallization of magma chambers [1]. Here, the point is to quantify to what extent the compositional and thermal convection influences the *in situ* crystallization, and, in particular, when heavy crystals formed at the upper (cooler) boundary stay in suspension due to convective motions until the full crystallization of the alloy. Another relevant application consists in understanding the dynamics of metal-silicate separation in a terrestrial magma ocean during the Earth's formation [2]. During the last accretion stage, most of Earth's mass and energy were acquired through the bombardment of the proto-Earth by planetesimals. Giant impacts released enough energy into proto-Earth to increase temperature by thousands of degrees. By fusion of the terrestrial surface, silicate magma oceans then appeared, through which metal droplets coming from the planetesimals had to settle to form the iron core of the Earth. One of our goals here is to quantify the influence of the turbulent thermal convection on this metal droplets scenario. Note finally that similar problems involving convection and sedimentation also appear in industrial settings, as, for instance, in the context of nano and microfluid heat transfer technologies, which have received increasing attention in recent years (see, for instance, [3]).

From a general point of view, the dynamics of turbulent flows containing dense suspended particles has been the subject of numerous studies. One of the fundamental papers is due to Wang and Maxey [4], who performed direct numerical simulations of this problem in isotropic homogeneous turbulence, including a one-way coupling (i.e., particles are advected by the flow field, but there is no back reaction on the carrier flow). They found that the terminal settling velocity of particles in the presence of turbulence is larger than the corresponding Stokes' velocity in a still fluid and explained this result by a preferential sweeping effect of the particles in downward moving fluid. Such a velocity enhancement by turbulence has then been qualitatively confirmed by experimental studies, using either a wind tunnel (e.g., [5]) or a tank with an oscillating grid (e.g., [6]). In contrast, the Monte Carlo computations by Mei [7], focusing on the nonlinear drag regime, exhibited a decrease in the mean particle settling velocity in the presence of turbulence. More recently, Bosse *et al.* [8] implemented a numerical study including a fully two-way coupling and confirm the settling velocity enhancement suggested by Wang and Maxey [4]. However, no quantitative agreement was found with experiments, leading the authors to ask for additional studies and collaborations between experimentalists and computational modelers on this still open question.

One of the problems in comparing experimental and numerical results comes from the use of periodic boundary conditions in numerical studies, which tacitly eliminates the possibility of particles re-entrainment from the bottom. This point was explicitly addressed by Huppert *et al.* [9], who demonstrated the importance of the bottom shear stress in the resuspension process. Confronting analytical models with their own experiments using grid-generated turbulence as well as with previous works, they concluded that the resuspension process strongly depends on the mechanisms for turbulence generation. In particular, significant differences are observed when turbulence is thermally driven since the relevant stress regarding particles-fluid interaction is then the buoyancy rather than the Reynolds stress (see also Solomatov *et al.* [10]). Specific studies devoted to the sedimentation of particles in the presence of vigorous convection are thus necessary.

*FAX: 33+ 4 96 13 97 09.
Email: lebars@irphe.univ-mrs.fr

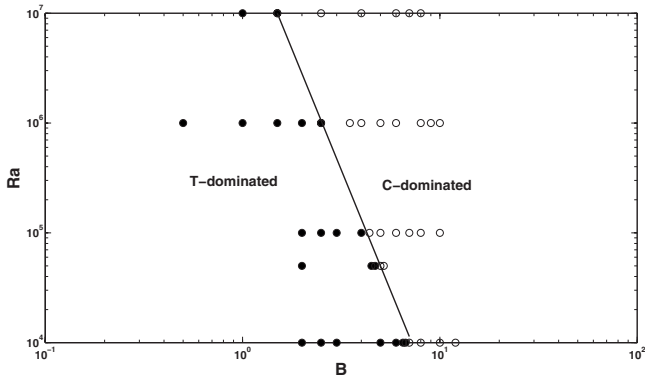

FIG. 1. Regime diagram in (B,Ra) determined numerically by Höink *et al.* [13] using two-dimensional computations at infinite Prandtl number with $R/H=1.6\times10^{-3}$. Filled circles stand for temperature-dominated cases and open circles for droplet-dominated cases. The separation between the two regimes is indicated by a straight line corresponding to our scaling law (13) with $\beta=0.77$ and $\mathrm{Pe}_s=3.5\times10^{-3}$.

However, up to now, only few papers have focused on this problem. From a numerical point of view, Gan *et al.* [11] performed direct numerical simulations of the sedimentation of one or two particles with thermal convection and found many effects of the convection on the trajectories and aggregation of particles. Koyaguchi *et al.* [12] conducted a series of experiments using a suspension of dense particles heated from below, focusing on the possible global regimes in the presence of a large initial mass fraction of suspended particles. They observed the formation of a density interface separating a dense convecting layer laden nearly uniformly with particles, from a clear layer without particles. Eventually, the hotter bottom layer becomes unstable, and a sudden overturn takes place, homogenizing the temperature and concentration. The whole process then starts again. Using a two-dimensional simulation at infinite Prandtl number, as well as a selected number of three-dimensional computations, Höink *et al.* [13] confirmed the existence of such an oscillating regime separating two cases: the temperature-dominated case ("*T* dominated"), where the droplets are advected by the flow and stay in suspension, and the droplet-dominated case ("*C* dominated"), where the convective motion is unable to keep the droplets suspended. According to their regime diagram reproduced in Fig. 1, the separation between the two cases depends (i) on the Rayleigh number $\mathrm{Ra}=\frac{\alpha_T g\Delta T H^3}{\nu\kappa}$, where g is the gravitational acceleration, H is the height of the tank, α_T is the fluid's thermal-expansion coefficient, ν is the kinematic viscosity, κ is the thermal diffusivity of the fluid, and ΔT the temperature drop across the tank, and (ii) on the buoyancy ratio $B=\frac{\Delta\rho}{\rho\alpha_T\Delta T}$, where $\Delta\rho$ is the difference between the density of the particles ρ_p and the density of the working fluid ρ. One must however notice that Höink *et al.* [13] only considered a one-way coupling, hence, limiting the validity of their results.

In the opposite limit of the low initial mass fraction of suspended particles, Martin and Nokes [1,14] described a laboratory model of the crystal settling in a vigorously convecting magma chamber. In following the time evolution of the number N of spherical polystyrene particles in suspension in a tank filled with convecting salty water, they concluded that in all their experiments, except one, N decays with time according to an exponential law $N=N_0\exp(-\frac{v_s t}{H})$. Here, N_0 is the initial number of particles in suspension, and v_s is the Stokes' velocity defined by $v_s=\frac{2}{9}\frac{\Delta\rho g R^2}{\eta}$, R is the radius of spherical particles, and η is the dynamical viscosity of the working fluid. In one of their experiments, i.e., in the one with the most viscous fluid and the smallest particles, Martin and Nokes [1,14] noticed that re-entrainment into plumes emerging from the bottom boundary layer occurred, so that the particle concentration approached a steady nonzero value at long time. By addition of a constant re-entrainment rate in their sedimentation equation, they managed to correctly fit the data coming from this special case. However, they did not systematically explore the dependence of this re-entrainment rate nor the mechanisms explaining its origin. Later on, using the same type of setup (i.e., aqueous solutions and polystyrene particles) but a different initial state (i.e., all particles are initially sedimented at the bottom of the tank), Solomatov *et al.* [10] studied analytically and confirmed experimentally the steady-state entrainment from a bed of particles by thermal convection. They argued that at the bottom of the tank, the tangential buoyancy stress can move the particles in the horizontal direction and build up dunes, from which the particles are then entrained in the bulk of the fluid. Using a systematic experimental study as well as the data from Martin and Nokes [1,14], they defined a critical value of the buoyancy stress nondimensionalized by $\Delta\rho gR$ separating a regime without particles bed motion from a regime of particles entrainment. Besides, Solomatov *et al.* [10] defined a scaling law describing the final solid fraction of particles in suspension, which they claimed to agree with their data. However, they did not exhibit systematic results, which leads Huppert *et al.* [9] to write that "the interpretation of these measurements is not so firmly supported as their earlier conclusions."

The present work takes place in the direct continuation of the studies by Martin and Nokes [1,14] and Solomatov *et al.* [10]. Using a similar experimental setup, we aim at combining and completing their results in systematically studying the re-entrainment process during particles sedimentation, starting from an initial homogeneous distribution of suspended particles through the whole tank. More specifically, in complement to the first experiment of Martin and Nokes [1,14] showing re-entrainment, we want to demonstrate that a constant re-entrainment coefficient is sufficient to explain the data for various values of the Rayleigh number Ra and of the density ratio $\Delta\rho/\rho$; in complement to the first results of Solomatov *et al.* [10], we want to systematically check the scaling of this re-entrainment coefficient with Ra and $\Delta\rho/\rho$.

II. EXPERIMENTAL SETUP

We study the sedimentation of spherical polymethyl methacrylate (PMMA) particles of radius $R=(300\pm25)$ μm and density $\rho_p=1.190$ in the presence of vigorous Rayleigh-Bénard convection. The working fluid consists in water with various amounts of salt NaCl to increase its density ρ (mea-

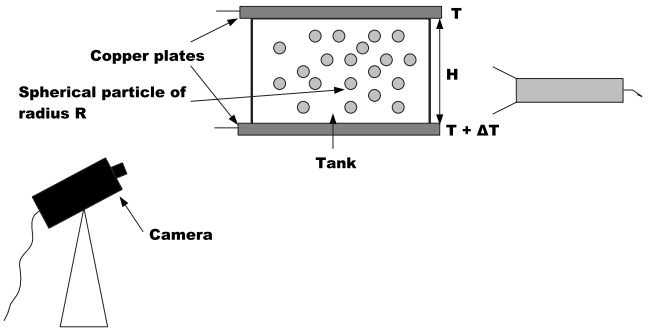

FIG. 2. Sketch of the experimental setup. The PMMA particles are shown as gray circles, much greater than in the reality.

sured at 20 °C) from 0.998 up to about 1.200. A sketch of the experimental setup is shown in Fig. 2. The tank (width 20×4 cm and height $H=20$ cm) is cooled from above and heated from below through two copper plates whose temperatures are imposed by two circulating thermostated baths and measured by thermocouples placed inside the plates. The tank is illuminated through its short side by a slide projector, so that the particles are clearly visible. The particles are initially distributed uniformly throughout the tank. To do so, we tested two methods. We first introduced the particles by the top. This method presents mainly three disadvantages. First, it necessitates to open the tank, which disrupts the thermal convection. Then, due to surface-tension phenomena, some particles stay at the surface. Finally, the PMMA particles are slightly porous: they can absorb up to 0.5% of water in volume and some molecules of salt can stay in the particles during the drying, changing their apparent density between two successive experiments. To minimize these effects, we choose to let the particles permanently in the salty water, in order to reach saturation. To distribute the particles uniformly through the tank, we initially stir the solution with a system of two magnets: one inside the tank and one outside. We then follow the statistical evolution of the number of suspended particles using a video camera and an image processing program written in MATLAB.

Our system is completely described by five dimensionless numbers: the Rayleigh number defined previously; the density ratio $\Delta\rho/\rho$, where $\Delta\rho=\rho_p-\rho$; the Prandtl number $\mathrm{Pr}=\frac{\nu}{\kappa}$, which compares the viscous and thermal diffusions; the aspect ratio R/H characterizing the relative size of the particles versus the typical size of the system; and finally the initial suspended solid fraction ξ_i. Note that the viscosity, the density, and the coefficient of thermal expansion of the fluid are temperature dependent. However, we are interested in the behavior of settling particles in the bulk of the convecting fluid, which is fully mixed and isothermal at the rather large Rayleigh numbers considered here, whereas temperature variations are limited to small thermal boundary layers close to the top and bottom plates. In the definition of the dimensionless parameters, we thus use the single value of the fluid parameters taken at the mean temperature of the tank. Note also that we use the density ratio here rather than the buoyancy number B defined in Höink *et al.* [13] because in our experiments, the control parameters are the temperature contrast and the water density: the density ratio and the Rayleigh

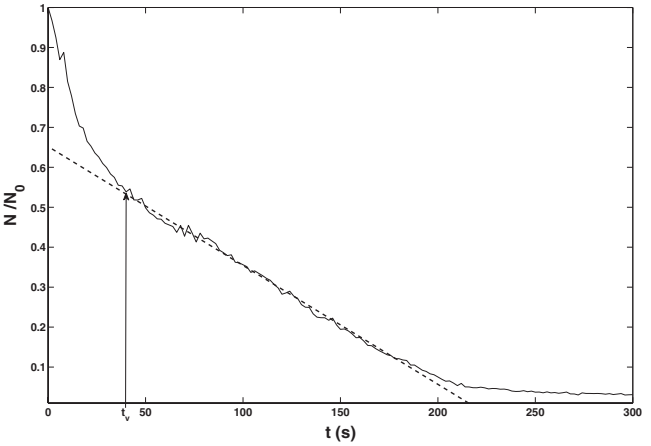

FIG. 3. Relative number of particles in suspension $\frac{N}{N_0}$ through time (in seconds) in the absence of convection ($\mathrm{Ra}=0$ and $\rho=1.184$). t_v corresponds to the viscous time of dissipation of the initial stirring. After t_v, simple sedimentation at the classical Stokes velocity takes place following our analytical law (2) (dashed curve).

number are thus controlled independently. In the present study, Ra typically ranges between 10^9 and 2×10^{10}, $\Delta\rho/\rho$ between 3×10^{-3} and 2×10^{-2}, and Pr between 3.5 and 14. The other dimensionless parameters are constant in our study, with $R/H=0.0015$ and a low value of the initial suspended solid fraction ξ_i of about 0.3%, ensuring that collective and hindered effects are negligible.

III. OBSERVATIONS AND MODELING

We first performed experiments without convection. As illustrated in Fig. 3, we systematically observed two stages in the evolution of the relative number of particles in suspension N/N_0 through time t. The first stage corresponds to the settling in the presence of motions due to the initial stirring, which tends to suspend and redistribute the particles. This stage vanishes after a typical viscous time t_v, corresponding to the typical time of dissipation of the initial eddies. t_v strongly depends on the characteristics of the stirring, especially on its characteristic length scale. So in all our experiments, we paid attention to reproduce the same initial stirring. After t_v, the particles settle at a constant velocity v_s and thus create a settling front. The conservation of the number of particles through time gives

$$N(t+dt)=N(t)-A\phi v_s dt \tag{1}$$

where A is the area of the base of the tank and ϕ is the particles volumic concentration. We verified experimentally that the distribution of particles under the front is quasiuniform and constant through time, so that $\phi=\frac{N_{t_v}}{AH}$ where $N_{t_v}=N(t=t_v)$ is the number of particles in suspension when the constant settling becomes predominant over the inertia of the initial stirring. Integration of Eq. (1) yields

$$N(t)=N_{t_v}\left[1+\frac{v_s}{H}(t_v-t)\right]. \tag{2}$$

Such a linear decay can be seen in Fig. 3, where we also show the result of the best fit of experimental data by Eq. (2),

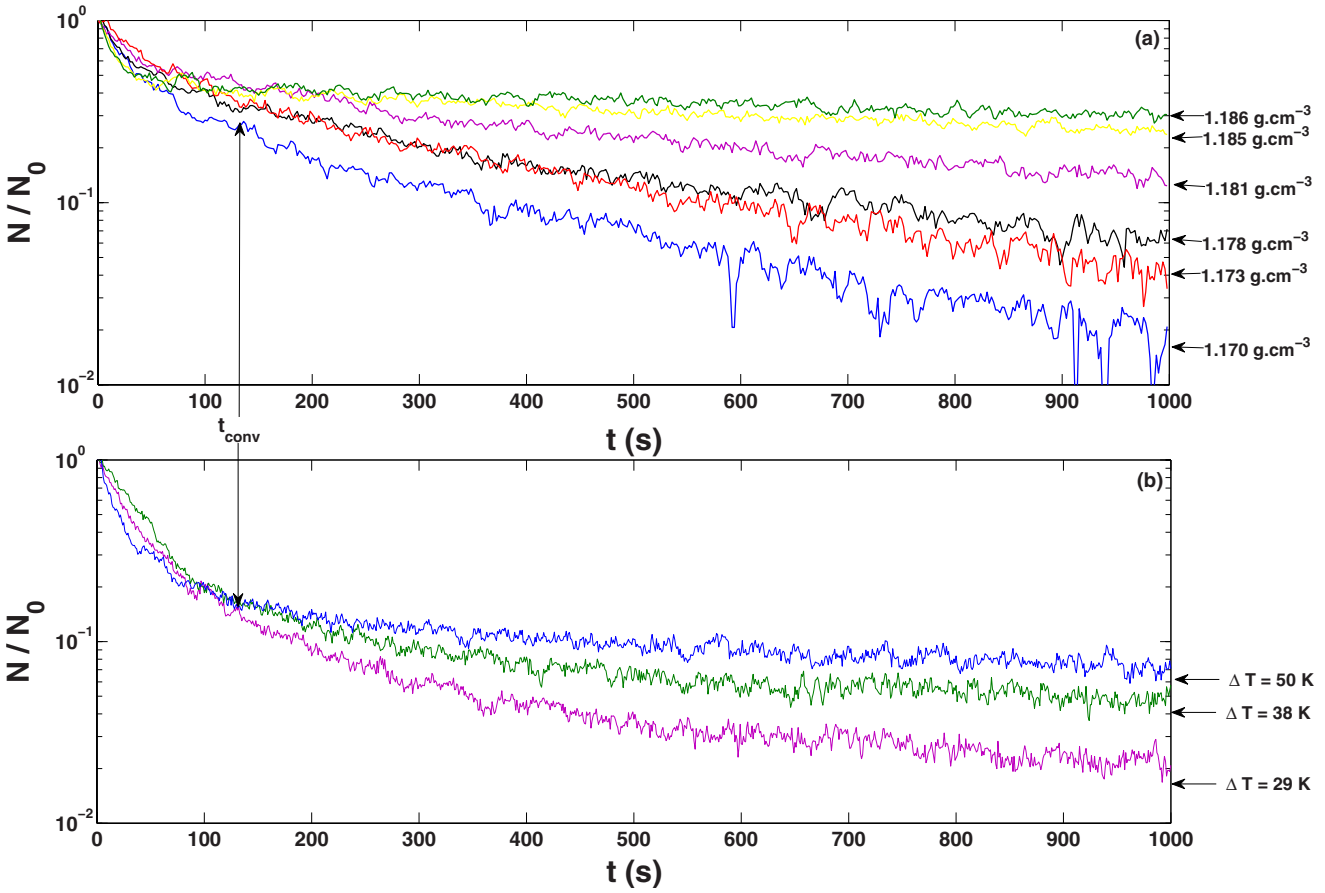

FIG. 4. (Color online) Relative number of particles in suspension $\frac{N}{N_0}$ through time (in seconds) in the presence of convection. (a) For a fixed value of the Rayleigh number ($\mathrm{Ra}=3\times10^9$) and various fluid densities (indicated on the right of the figure) and (b) for a fixed value of fluid density $\rho=1.150$ and various Rayleigh numbers (see the temperature contrasts ΔT indicated on the right part of the figure). Initially, all curves overlap because of the inertia of the mechanical stirring. After the time t_{conv} corresponding to the reappearance of the convection motions, the evolution of $\frac{N}{N_0}$ strongly depends on $\frac{\Delta\rho}{\rho}$ and on ΔT. Note that the noisiness of the data is due to both real statistic fluctuations on the large number of suspended particles as well as to the measurements artifact related to our image processing.

taking t_v and v_s as adjustable parameters (dashed curve). In all our experiments without convection, we systematically find an experimental value of v_s in good agreement with Stokes' formula, with a mean relative uncertainty of 17%, which we attribute to the dispersion in the particles sizes.

Typical time evolutions of the relative number of particles in suspension N/N_0 in the presence of convection are shown in Fig. 4 for various values of the temperature and density contrasts. As in experiments without convection, we systematically observe a first stage related to the initial stirring. The sedimentation during this first stage seems to be independent of the temperature contrast. Convective motions then reappear. For the typical Rayleigh numbers reached in this study (i.e., about 10^9), one can model the flow inside the tank in three different layers: an isothermal bulk, where turbulent convective motions take place and two symmetric thermal boundary layers of depth δ_{th} (one at the top and one at the bottom), where heat transfer is purely diffusive. Following the classical study by Howard [15], the scaling of δ_{th} is determined by the fact that the local Rayleigh number computed on a thermal boundary layer with a temperature contrast $\Delta T/2$ is critical. Hence,

$$\delta_{th} = H\left(\frac{2\mathrm{Ra}_c}{\mathrm{Ra}}\right)^{1/3}, \tag{3}$$

where Ra_c is the critical Rayleigh number, about 1708 in our case. Convective motions in the bulk come from the emergence of thermal plumes from both boundary layers. The typical convective time separating the emergence of two plumes at the same location, also characterizing temperature fluctuations in the bulk, corresponds to the typical time necessary to establish the temperature contrast inside the boundary layer by diffusion, hence,

$$t_{th} = \frac{\delta_{th}^2}{\pi\kappa} = \frac{H^2}{\pi\kappa}\left(\frac{2\mathrm{Ra}_c}{\mathrm{Ra}}\right)^{2/3} \approx 10s. \tag{4}$$

One can notice that the viscous dissipation time of initial eddies t_v in the absence of convection and the typical convective time t_{th} are close. This explains why in our experiments, the disappearance of the initial mechanical stirring as well as the reappearance of convective motions take place almost simultaneously. Note finally that the typical convec-

tive velocity is simply given by $v_c = \delta_{th}/t_{th} = \pi\kappa/H(\mathrm{Ra}/2\mathrm{Ra}_c)^{1/3}$.

Once convection is fully established, the statistical behavior of suspended particles strongly depends on $\Delta\rho$ and ΔT (Fig. 4): the characteristic time of settling as well as the final proportion of particles in suspension significantly increase when either ΔT increases or $\Delta\rho$ decreases, as expected.

Seen from a particle frame, the convective turbulent velocity field of the flow appears as isotropic and tends to disperse the particles. So, this phenomenon can be modeled by a classical diffusion process [16] outside the thermal boundary layers, where no convective motion takes place. The conservation equation for particles in the bulk of the fluid, after averaging in the horizontal directions x and y, then writes

$$\frac{\partial\phi}{\partial t} - v_s\frac{\partial\phi}{\partial z} - D\frac{\partial^2\phi}{\partial z^2} = 0, \tag{5}$$

valid after the reappearance of the turbulent convection at t_{conv} (i.e., typically after some t_{th}). Here, v_s is the sedimentation velocity and D is a turbulent convective diffusion coefficient. By integration of Eq. (5) between δ_{th} and $H-\delta_{th}$ (i.e., the convecting part of the flow), we obtain

$$\frac{1}{A}\frac{dN}{dt} - v_s[\phi(H-\delta_{th}) - \phi(\delta_{th})] - D\left[\left(\frac{\partial\phi}{\partial z}\right)_{H-\delta_{th}} - \left(\frac{\partial\phi}{\partial z}\right)_{\delta_{th}}\right] = 0. \tag{6}$$

Following the study of Belinsky *et al.* [17], we consider that there is no transport of particles through the upper boundary layer, so that the total particulate flux is equal to zero for $z = H-\delta_{th}$. Besides, we systematically observe in our experiments that the concentration in the bulk is quasiuniform, so that $\phi(\delta_{th}) \approx N/AH$. Hence,

$$\frac{dN}{dt} + \frac{v_s N}{H} = -DA\left(\frac{\partial\phi}{\partial z}\right)_{\delta_{th}}. \tag{7}$$

The right-hand side term of this equation corresponds to the diffusive flux at the interface between the bottom thermal boundary layer and the bulk. Following the initial suggestion of Martin and Nokes [1,14], we assume that this flux, which actually corresponds to the number of particles, which are resuspended per unit time R_{conv}, is constant. We expect this to be true as long as the amount of deposited particles is large enough for the bottom boundary layer never to be fully depleted at any time. This is indeed the case in all our experiments once convective motions have reappeared. Once the statistical stationary state is reached, $\frac{dN}{dt}=0$ and N takes a constant equilibrium value N_{eq}, so that $R_{conv}=\frac{v_s N_{eq}}{H}$. Finally,

$$\frac{dN}{dt} + \frac{v_s N}{H} = R_{conv} = \frac{v_s N_{eq}}{H}, \tag{8}$$

which yields to

$$N(t) = (N_{t_{conv}} - N_{eq})\exp\left[-\frac{v_s}{H}(t-t_{conv})\right] + N_{eq}, \tag{9}$$

where $N_{t_{conv}} = N(t=t_{conv})$ is the initial number of suspended particles once convective motions reappear. This simple equation allows us to correctly describe all our experiments, taking N_{eq} and v_s as adjusting parameters depending on Ra and $\frac{\Delta\rho}{\rho}$. An example of the temporal evolution of the number N of particles in suspension in the presence of convection ($\mathrm{Ra}=3\times10^9$ and $\rho=1.186$) is shown in Fig. 5, together with the result of the best fit by Eq. (9), valid for $t > t_{conv} \sim 50s$.

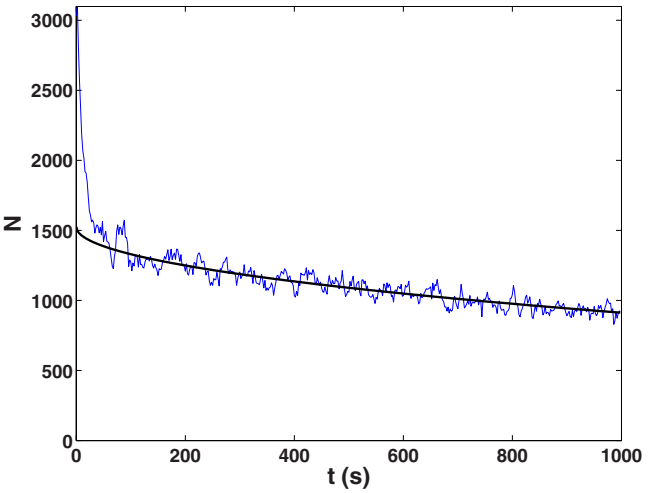

FIG. 5. (Color online) Temporal evolution of the number N of particles in suspension in the presence of convection ($\mathrm{Ra}=3\times10^9$ and $\rho=1.186$). The continuous line represents the data fitting according to Eq. (9), valid for $t > t_{conv}$.

Figure 6 shows the systematic evolution of the settling velocity v_s determined experimentally as a function of $\Delta\rho/\rho$ for a fixed value of the Rayleigh number $\mathrm{Ra}=3\times10^9$ and for a fixed mean temperature of 25 °C. Values of v_s correspond to indirect data, coming from the fitting of experimental measurements by Eq. (9). Besides, our setup does not allow to explore a very large range in $\Delta\rho/\rho$. Hence, we do not try here to define an experimental scaling law expressing its de-

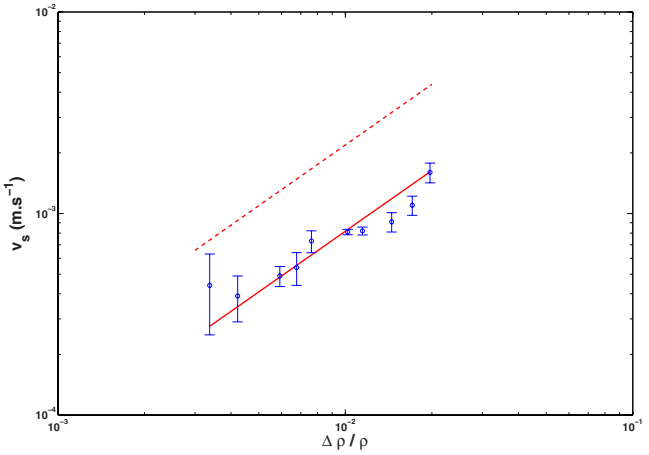

FIG. 6. (Color online) Sedimentation velocity determined experimentally using Eq. (9) versus $\frac{\Delta\rho}{\rho}$ for $\mathrm{Ra}=3\times10^9$. The experimental data correspond to the classical Stokes velocity, providing that we consider an apparent viscosity of 2.4×10^{-6} $\mathrm{m^2\,s^{-1}}$ (continuous line). The dashed line shows the calculation of the Stokes velocity with a molecular kinematic viscosity 10^{-6} $\mathrm{m^2\,s^{-1}}$, valid without convection.

pendence on $\Delta\rho/\rho$, but we rather test the compatibility of our results with relevant analytical models. Here, we observe that the experimental results are compatible with a linear dependence in $\frac{\Delta\rho}{\rho}$, which would derive from the classical Stokes' velocity. However, the experimental prefactor is smaller than the theoretical one using the kinematic "molecular" viscosity at 25 °C $\nu=0.896\times10^{-6}$ m^2 s^{-1} (dashed line), which nevertheless was relevant to explain our experiments without convection. This could be explained by the fact that at the typical Rayleigh numbers considered here, the turbulence is fully developed and the apparent viscosity seen by the particles corresponds to the molecular viscous dissipation on their solid surface by all small-scale eddies (i.e., smaller than the particles). Such a method consisting in describing large scale motions inside a turbulent fluid by a laminar law using an apparent viscosity was already successfully used by Brito *et al.* [18] when studying the spin up of a rotating fluid in the presence of turbulent convection: they then measured $1.16<\nu_a/\nu<1.49$ for $24.1<\mathrm{Ra}/\mathrm{Ra}_c<78.2$. In the case shown in Fig. 6 at $\mathrm{Ra}=3\times10^9\sim10^6\mathrm{Ra}_c$, we find a typical value $\nu_a/\nu=2.7$. This result suggests that the dependence of ν_a in Ra is weak, corresponding to a 2.7 increase over 6 orders of magnitude in Ra. Since our setup only allows to explore the range $[10^9;2\times10^{10}]$ in Ra, we do not expect to observe any systematic variations of ν_a as a function of Ra. Note also that we do not expect the apparent viscosity measured here to be directly related to the turbulent viscosity of numerical models of turbulence, which characterizes the transport and dissipation of energy by the fluctuations of the flow and is thus independent of the molecular viscosity.

Using our systematic experimental results, we also study the variations in the equilibrium number of particles N_{eq}. To obtain a result independent of the size of the system, we rather seek for a scaling law characterizing the equilibrium volume fraction of particles $\xi_{eq}=\frac{V_p}{V_{obs}}N_{eq}$, where $V_p=\frac{4}{3}\pi R^3$ is the volume of one particle and V_{obs} is the observed volume. The energy necessary for maintaining heavy particles in suspension can only come from the work of viscous friction at their surface. The statistically stationary state is reached when the energy usually lost by viscous friction inside the convecting fluid is sufficient to compensate for the potential energy accumulated in the suspended heavy particles, i.e.,

$$\int\int\int_{all\ particles}\vec{v}_s\cdot\Delta\rho\vec{g}dV\sim\int\int\int_{V_{obs}}\vec{v}_c\cdot\eta\nabla^2\vec{v}_c dV. \tag{10}$$

In term of orders of magnitude, this writes

$$v_s\Delta\rho g\xi_{eq}V_{obs}=\epsilon v_c\eta\frac{v_c}{l^2}V_{obs}, \tag{11}$$

where ϵ is a constant of order 1 to be determined experimentally, l is the typical length scale of convective motions, which we take as the thermal length δ_{th}, and v_c is the typical convective velocity introduced above. After simplification, we obtain

$$\xi_{eq}=\epsilon\frac{9\pi^2}{2}\frac{\kappa^2\nu_a\nu}{H^4g^2R^2}\left(\frac{\mathrm{Ra}}{\mathrm{Ra}_c}\right)^{4/3}\left(\frac{\Delta\rho}{\rho}\right)^{-2}. \tag{12}$$

This scaling law is similar, except for a constant multiplicative factor that can be included in ϵ, to the one determined by Solomatov *et al.* [10], coming from the equilibrium between the heat flux related to convection and the potential energy of suspended particles, taking into account an "efficiency factor" of energy conversion. Figure 7(a) shows the evolution of ξ_{eq} determined experimentally as a function of $\Delta\rho/\rho$. As for the study of v_s, ξ_{eq} is an indirect data coming from the fitting of experimental measurements by Eq. (9) and the explored range is relatively small. Hence, we do not try to define an experimental scaling law expressing its dependence on $\Delta\rho/\rho$, but we rather test the compatibility of our results with our analytical model, given by Eq. (12). As shown in Fig. 7(a), a slope (−2) is indeed compatible, and the corresponding prefactor allows us to calculate ϵ, giving $\epsilon\approx0.25$ with $\nu_a=2.4\times10^{-6}$ m^2 s^{-1}. Similarly, Fig. 7(b) shows the variations of ξ_{eq} as a function of $\nu_a\nu(\mathrm{Ra}/\mathrm{Ra}_c)^{4/3}(\Delta\rho/\rho)^{-2}$ derived from series of experiments, where the bottom temperature has been systematically changed for a given fluid. Our data validate the scaling law (12), with a value of $\epsilon\approx0.54$, of the same order of magnitude as the previous value. Note however that the uncertainty on ϵ is large. To compare these values with the efficiency factor defined by Solomatov *et al.* [10], we simply have to multiply ϵ by $\frac{2\pi^2}{\mathrm{Ra}_c}$. We then obtain efficiency values between 0.3% and 0.6%, in good agreement with the estimations of Solomatov *et al.* [10], which range between 0.2% and 0.9%.

IV. CONCLUSIONS

Our systematic experimental study confirms the first experiment by Martin and Nokes [1]: a constant re-entrainment term, derived from the introduction of a turbulent convective diffusive flux of particles from the bottom, allows to correctly describe the settling of initially randomly distributed heavy particles in the presence of vigorous convection. We also confirm that this re-entrainment term follows the scaling law suggested by Solomatov *et al.* [10] for the entrainment from a bed of particles. Besides, our systematic experimental results demonstrate that the mean particles settling velocity scales as the classical Stokes velocity (i.e., linear dependence in $\frac{\Delta\rho}{\rho}$), providing that the fluid molecular viscosity is replaced by an apparent viscosity, which corresponds to the integration of all molecular viscous dissipations by small-scale eddies at the surface of a particle. Clearly, additional studies regarding this apparent viscosity are necessary, allowing in particular the exploration of a larger range of Rayleigh numbers and a systematic study of its variations with the particles diameter and the fluid viscosity. But in any case, the first trends shown here demonstrate that the fluid dynamics of the metal droplets sedimentation in a primitive magma ocean should not be oversimplified on the simple basis of the large density difference between iron and silicate. In particular, we claim that a typical value of the settling velocity found in the literature (i.e., $v_s\sim0.5$ m/s [2]), which is especially important since it determines the typical time for

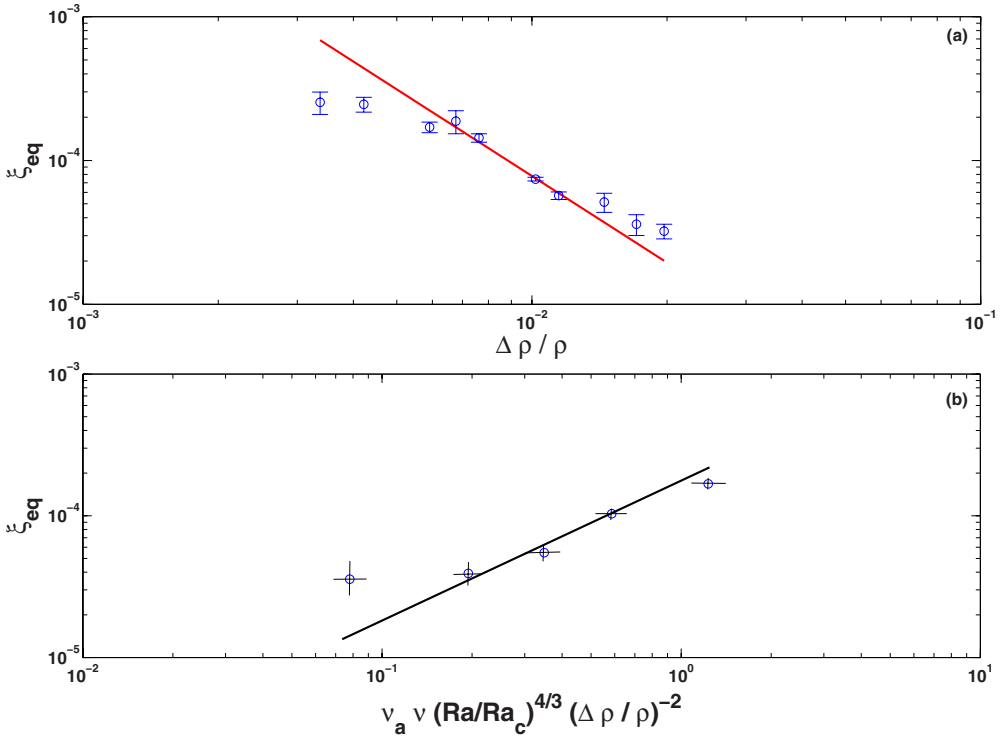

FIG. 7. (Color online) Equilibrium suspended volume fraction ξ_{eq} measured experimentally, (a) as a function of $\frac{\Delta\rho}{\rho}$ for a fixed $\mathrm{Ra}=3\times10^9$ and (b) as a function of the factor $\nu_a\nu(\mathrm{Ra}/\mathrm{Ra}_c)^{4/3}(\Delta\rho/\rho)^{-2}$ suggested by our scaling law (12), when systematically changing the bottom temperature of our tank for a given fluid of density $\rho=1.150$ at 25 °C. Lines correspond to the theoretically predicted dependence according to the scaling law (12), with a slope −2 in $\frac{\Delta\rho}{\rho}$ and a slope 1 in $\nu_a\nu(\mathrm{Ra}/\mathrm{Ra}_c)^{4/3}(\Delta\rho/\rho)^{-2}$. We also assume that the ratio ν_a/ν is constant and equal to 2.7.

chemical equilibration of metal droplets with their silicate environment, is probably overestimated. For illustration purpose only, if we suppose that the apparent viscosity follows a power law $(\nu_a/\nu)\sim(\mathrm{Ra}/\mathrm{Ra}_c)^p$ and if we determine the constant exponent p using our experimental result, we find $p\sim0.06$. For the typical Rayleigh number of a primitive magma ocean, ranging between 10^{28} and 10^{32} [2], we thus predict an increase in viscosity by a factor ranging between 31–55. However, in any case, the equilibrium suspended fraction predicted by Eq. (12) always remains negligible, as expected from geochemical observations.

To finish with, in addition to these conclusions valid in the limit of small initial volume fraction of suspended particles (see, for instance, [12]), it is interesting to note that our description in terms of convective diffusive flux of particles [Eq. (5)] also explains the regime diagram of Höink *et al.* [13] shown in Fig. 1. Indeed, Eq. (5) leads to define a Peclet number $\mathrm{Pe}=\frac{v_s H}{D}$ distinguishing two regimes: when $\mathrm{Pe}\ll\mathrm{Pe}_s$, where Pe_s is a constant critical Peclet number to be determined, the turbulent diffusion is predominant and the particles stay in suspension, corresponding to the T-dominated case introduced by Höink *et al.* [13]. On the contrary, the particles settle when $\mathrm{Pe}\gg\mathrm{Pe}_s$, corresponding to the C-dominated case. By analogy with the Einstein's model of Brownian motions, we estimate the turbulent convective diffusion coefficient $D=v_c\times H$, where H is the mean free path of convective motions, $v_c=\frac{\pi\kappa}{H}(\frac{\mathrm{Ra}}{\mathrm{Ra}_c})^\beta$ is the typical convective velocity, and β is a constant exponent depending on the flow characteristics (see, for instance, [19]). Then, the Peclet number simply corresponds to the ratio between the sedimentation and the convective velocities. The separation between the two regimes in a (B,Ra) diagram is given by the equation

$$\mathrm{Pe}_s=\frac{2}{9\pi}\mathrm{Ra}_c^\beta\left(\frac{R}{H}\right)^2 B\mathrm{Ra}^{1-\beta}. \tag{13}$$

The best fit of this equation with the numerical results of Höink *et al.* is shown in Fig. 1 and gives $\beta=0.77$ and $\mathrm{Pe}_s=3.5\times10^{-3}$. This value $\beta=0.77$ is compatible with the scaling of the convective velocity in the same numerical configuration, i.e., two dimensional and at $\mathrm{Pr}=\infty$ (see, for instance, Korenaga and Jordan [20]).

ACKNOWLEDGMENTS

The authors acknowledge helpful discussions with E. Guazzelli, L. Bergougnoux, and O. Marc.

[1] D. Martin and R. Nokes, Nature (London) **332**, 534 (1988).
[2] D. C. Rubie, H. Melosh, J. Reid, C. Liebske, and K. Righter, Earth Planet. Sci. Lett. **205**, 239 (2003).
[3] B. H. Chang, A. F. Mills, and E. Hernandez, Int. J. Heat Mass Transfer **51**, 1332 (2008).
[4] L. P. Wang and M. Maxey, J. Fluid Mech. **256**, 27 (1993).
[5] A. Aliseda, A. Cartellier, F. Hainaux, and J. C. Lasheras, J. Fluid Mech. **468**, 77 (2002).
[6] T. S. Yang and S. S. Shya, Phys. Fluids **15**, 868 (2003).
[7] R. Mei, Int. J. Multiphase Flow **20**, 273 (1994).
[8] T. Bosse, L. Kleiser, and E. Meiburg, Phys. Fluids **18**, 027102 (2006).
[9] H. Huppert, J. S. Turner, and M. Hallworth, J. Fluid Mech. **289**, 263 (1995).
[10] V. Solomatov, P. Olson, and D. Stevenson, Earth Planet. Sci. Lett. **120**, 387 (1993).
[11] H. Gan, J. Chang, J. Feng, and H. Hu, J. Fluid Mech. **481**, 385 (2003).
[12] T. Koyaguchi, M. Hallworth, H. Huppert, and R. S. Sparks, Nature (London) **343**, 447 (1990).
[13] T. Höink, J. Schmalzl, and U. Hansen, Geochem. Geophys. Geosyst. **7**, Q09008 (2006).
[14] D. Martin and R. Nokes, J. Petrol. **30**, 1471 (1989).
[15] L. Howard, in *Proceedings of the 11th International Congress on Applied Mechanics*, edited by H. Görtler (Springer, New York, 1964), pp. 1109–1115.
[16] F. Blanchette, M. Strauss, E. Meiburg, B. Kneller, and M. E. Glinsky, J. Geophys. Res. **110**, C12022 (2005).
[17] M. Belinsky, H. Rubin, Y. Agnon, E. Kit, and J. Atkinson, Environ. Fluid Mech. **5**, 415 (2005).
[18] D. Brito, J. Aurnou, and P. Cardin, Phys. Earth Planet. Inter. **141**, 3 (2004).
[19] S. Grossmann and D. Lohse, J. Fluid Mech. **407**, 27 (2000).
[20] J. Korenaga and T. Jordan, Geophys. J. Int. **147**, 639 (2001).